SLAC – PUB – 4633
May 1988
(T/E)

A NOTE ON COLOR MAGNETISM MODELS AND THE ELECTROPRODUCTION OF THE Δ (1232)*

OSCAR A. RONDON–ARAMAYO
Department of Physics, INPP,
University of Virginia, Charlottesville, VA 22901
and
Stanford Linear Accelerator Center,
Stanford University, Stanford, CA 94309

ABSTRACT

In this work the author discusses the experimental consequences of the use of the color magnetism concept in nonrelativistic quark models of the nucleon and its resonances. It is found that recent prescriptions used by some authors to apply this model to calculate amplitudes for the photoproduction and electroproduction of the Δ (1232) resonance do not give satisfactory agreement with well-established experimental results for the $\gamma N \to \Delta$ or $\gamma_v N \to \Delta$ processes. Some of the reasons for the disagreement are considered and an alternative approach is suggested.

Submitted to Nuclear Physics A

*Work supported by the Department of Energy, contracts DE–AC03–76SF00515 and DE–FG0586ER40261.

1. Introduction

The idea of color magnetism as an additional component of the quark-quark interaction, introduced by De Rújula, Georgi and Glashow,[1] implied the appearance of contact and tensor forces (hyperfine interaction) between quark pairs, leading to the possibility of having in the ground state baryons (e.g., nucleon, delta, etc.) instances of mixed symmetry states, as well as mixing of higher orbital angular momentum waves (P and D waves) in addition to the usual S waves. The former waves would also represent a deformation of the quark charge or mass distributions, which in the case of the nucleon and the Δ (1232) would imply a breaking of the spherical symmetry required by SU(6).

Several authors[2] have applied this concept within the framework of the constituent quark model to calculate the values of the electromagnetic transition amplitudes for the $\gamma N \to N^*$ process, in particular for those that become non-zero when deformed baryon wave functions are introduced. The relevant amplitudes related to the photoproduction (with real or virtual photons) of the nucleon resonances, specifically the Δ (1232), are the multipoles $E_{\ell\pm}, M_{\ell\pm}$, $L_{\ell\pm}$ or equivalently the helicity amplitudes $A_{3/2}, A_{1/2}, A_0$. Only s and p waves contribute significantly to pion photoproduction and electroproduction in the invariant mass region of the Δ (also known as the $P_{33}(1232)$, or P'_{33} in the earlier notation). This restriction implies that only $\ell \leq 1$ multipoles are considered, and among those, only the E_{1+}, M_{1+} and L_{1+} are associated with the resonant part of the γN scattering process.

While numerous predictions for the electric quadrupole E_{1+}, the magnetic dipole M_{1+} and their ratio (E2/M1, in nuclear physics notation) formulated in a variety of quark and phenomenological models have been published, only a few among them apply the concept of color magnetism, including explicitly the contributions of D states in the nucleon and Δ wave functions.[3] Moreover, there are only two or three predictions of any kind for L_{1+}[4] (and the related scalar multipole S_{1+}).

In this paper, we will attempt to extract the experimentally useable information resulting from the predictions of the color magnetism models that involve D states, for the magnitudes and Q^2 dependence of the multipole amplitudes, and to suggest ways to interpret the sources of the discrepancies with the accepted experimental values for these quantities.

2. The E_{1+}, M_{1+} Multipoles and the E2/M1 Ratio in Δ Photoproduction

We begin our comparison with the E2/M1 ratio for photoproduction ($Q^2 = 0$). Table I presents the results of three versions of the color magnetism model for this quantity.

In all instances, the authors used a nonrelativistic harmonic oscillator for the interquark potential, to which they added the corresponding electromagnetic interaction Hamiltonian for the γ absorption. The main differences between them are the inclusion by Gershtein and Dzhikiya (G–D) of the small P wave antisymmetric state for the nucleon, and the addition by Weber and Williams of an OPEP potential, to represent the effects of meson exchange between quarks. It is clear that significantly different results are obtained even when the authors use the same model. Moreover, in the three cases that rely on pure color magnetism, the ratio seems to be underestimated, as compared with the experimental value.

If we examine in greater detail the quantities that make up the ratio, we find that only G–D have actually calculated E_{1+} and M_{1+}.* They obtained $E_{1+} = -6.6 \times 10^{-3} N$ and $M_{1+} = 2.07 N$. The meaning of N is detailed in the appendix, where we also give the full analytical expressions for the multipoles. When these results are translated to the usual units of inverse π^+

* Bourdeau and Mukhopadhyay (B–M) use G–D's M_{1+} value to calculate their ratio, invoking also the Siegert theorem to take $E_{1+}(Q^2 = 0) \simeq S_{1+}(Q^2 = 0)$, where $-Q^2[\mathrm{GeV/c}]^2$ is the photon's four-momentum transfer squared. We mention in passing that these authors have also used the deformed bag model of Vento et al.,[3] which we don't review here because of its even greater discrepancies with experiment.

masses for the multipole amplitudes, these authors find that at resonance $E_{1+} \approx -0.055i(10^{-3}\ m_{\pi^+}^{-1})$ and $M_{1+} \approx 17i(10^{-3}\ m_{\pi^+}^{-1})$ for the $\pi^o p$ decay channel. A comparison with the best fits to the experimental pion photoproduction data,[5] reveals a marked disagreement, as we present in Table II.

The existence of discrepancies between the color magnetism estimates of the multipoles and the experimental results, was pointed out by G–D, who in their work indicated that the color magnetic M_{1+} is smaller than the corresponding SU(6) prediction, as a consequence of the symmetry breaking tensor forces. However M_{1+} was already underestimated in SU(6) to be less than 88% of the experimental value.[6]

To conclude this section we present in Table III the results for the helicity amplitudes which are the primary quantities calculated in the models and from which the multipoles are computed. It is clear from these figures that the ability of a model to reproduce an approximation of the E2/M1 ratio means nothing more than the model's satisfying a necessary but certainly not a sufficient condition for correctness.

3. Electroproduction and the Resonant Multipoles

We have seen in the previous section that "pure" color magnetism, as applied by some authors (notably G–D) to the prediction of the magnitudes of the Δ photoproduction amplitudes, shows significant deficiencies. To investigate further where the problem lies, in this section we will extend our study to the $Q^2 \neq 0$ region, where the Coulomb (S_{1+}) or longitudinal (L_{1+}) multipoles can also contribute to the total resonant transition cross section, in addition to M_{1+} (which is the dominant mode) and E_{1+}.

To this effect, we initially follow the methodology used by B–M to obtain the Q^2 dependence of each of the four multipoles M_{1+}, E_{1+}, L_{1+} and S_{1+}. For the first two, they modified the corresponding photoproduction transition operators given by G–D,[2] by replacing the coefficient $(2\pi/|\mathbf{q}^*|)^{1/2}$ in the expression for the radiation potential, by a factor $(2\pi/K_0)^{1/2}$, where $K_0 = (M_R^2 - M^2)/2M_R$. M_R and M are the masses of the $\Delta^+(1.2318[\mathrm{MeV/c^2}]$, from Berends and Donnachie[5]) and of the proton, respectively. Obviously, $|\mathbf{q}^*||_{Q^2=0} \equiv K_0$.

On the other hand, for L_{1+} and S_{1+}, they derived expressions of their own, starting from the longitudinal and scalar helicity amplitudes for zero photon helicity. This procedure leads to two separate ways of calculating L_{1+}: directly, from the "current" or longitudinal operator; and from the "charge" or scalar operator, by way of its current conservation relation to S_{1+}.

In the remainder of this section we will review the correct form of reproducing B–M's results and we will compare them with well-established experimental values, while in the last section we will discuss the possible reasons for the discrepancies that are found. The results are presented in two parts, for E_{1+}, L_{1+} and S_{1+}, and for M_{1+}, respectively. The reasons for this separation are based on the quality of the available experimental data, as we will see below.

The Q^2 dependecies of S_{1+}, L_{1+} and E_{1+}, obtained by the present author using G–D's and B–M's equations as input are shown in fig. 1(a), for the Q^2 range from $-0.2[\mathrm{GeV/c}]^2$ (unphysical) to $4[\mathrm{GeV/c}]^2$. The reason for the extension to negative Q^2 is displayed more clearly in fig. 1(b) where the low Q^2 region is enlarged for the purpose of showing the behavior of the multipoles at $|\mathbf{q}^*| = 0$. (corresponding to $Q^2 = -0.0864[\mathrm{GeV/c}]^2)$. Several features of the plot deserve to be remarked:

- All multipoles converge to 0 at $|\mathbf{q}^*| = 0$. Thus, the condition $Lim_{|\mathbf{q}^*|\to 0}$ $E_{1+}/L_{1+} = 1$[7] is satisfied, although in a forced fashion (0/0 may or may not be equal to 1).

- $L_{1+\rho}$ and L_{1+j} converge to 0 but following very different paths. This emphasizes the contrast between the two ways of calculating L_{1+} and the effects of truncating the oscillator level scheme at $n = 2$ as pointed out by Drechsel and Giannini.[2]

- An extension of the Siegert theorem[8] was invoked by B-M to equate E_{1+} and S_{1+} at $Q^2 = 0$. It is clear, however, that this theorem is not fulfilled except at the unphysical value $|\mathbf{q}^*| = 0$. This deficiency was already noted by those authors who, nevertheless, used the theorem to conclude that the sign and order of magnitude of the ratio E2/M1 ($\simeq S_{1+}/M_{1+}$) agree with experiment at the photoproduction point.

- In all cases the negative exponential dependence of the normalization coefficient effectively suppresses the multipoles at $Q^2 \simeq 4[\mathrm{GeV/c}]^2$. This result applies to M_{1+} as well (see fig. 4), and it could explain the observed reduction of the resonance peak with increasing Q^2. As noted by Foster and Hughes,[9] however, this decrease is faster than the expected dipole form factor. We note in passing that fig. 2 of B–M's paper displays an incorrectly plotted version of the L_{1+j} multipoles, as our fig. 2 shows.

The limited experimental data on the longitudinal (or scalar,) and electric quadrupole moments for electroproduction and photoproduction of the Δ make any comparison a very difficult task, because a clear distinction between the predictions of models and the measured quantities can be achieved only in some exceptional cases. However, the magnetic dipole M_{1+} (and its derived quantities, the magnetic transition form factor G_M^* and the resonant inclusive transverse cross section σ_T,) plays a dominant role in the transition, to the extent that the data available for it at the resonant mass are quite accurate.[10] In fig. 3 we can see that, besides the difference at $Q^2 = 0$ discussed earlier, substitution of M_{1+} (calculated from the model in the same fashion as the other multipoles) in the well-known relation

$$G_M^{*2}(Q^2) = \frac{4M^2\Gamma|\mathbf{k}^*|}{\alpha|\mathbf{q}^*|}|M_{1+}^{3/2}(Q^2)|^2 \tag{1}$$

leads to a ratio G_M^*/G_D that is very different from the experimentally observed one, with M_{1+} taken as purely imaginary at resonance. In fact, not even an approximate dipole decrease is seen, but rather a peak at $Q^2 \simeq 0.9[\mathrm{GeV/c}]^2$, an effect that implies growth of the resonance cross-section with increasing Q^2.

Figure 4 illustrates precisely this effect, for the inclusive transverse cross section. The theoretical line was obtained by assuming dominance of the resonant M_{1+} and E_{1+} multipoles, replaced in the following experimental expression:*

$$\sigma_T = 4\pi \frac{|\mathbf{k}^*|W}{KM} \left(2|M_{1+}|^2 + 6|E_{1+}|^2\right) \quad . \tag{2}$$

Here W represents the resonances's invariant mass and K is the laboratory system equivalent of K_0, while here as well as in eq. (1), $|\mathbf{k}^*|$ is the pion momentum in the γN c.m. system. The experimental points are the resonant part of the cross section obtained by the usual decomposition of the inclusive cross-section into a Breit–Wigner shape plus a background. The ratio σ_S/σ_T illustrates the relative importance of the scalar(longitudinal) resonant cross section. It was calculated from

$$\sigma_S/\sigma_T = \frac{Q^2}{|\mathbf{q}^*|^2} \frac{8|S_{1+}|^2}{2|M_{1+}|^2 + 6|E_{1+}|^2} \cong 4 \frac{Q^2}{|\mathbf{q}^*|^2} \frac{|S_{1+}|^2}{|M_{1+}|^2} \quad . \tag{3}$$

4. Conclusions and Alternative Approach

We conclude that reproducing the ratios of the photoproduction amplitudes says little about the overall validity of the model. In fact, unless some significant corrections are introduced, the disagreement with experiment indicates that color magnetism in its current version and in its application to the electromagnetic properties of the baryons developed by G–D and B–M, is an insufficient mechanism to reproduce the observed magnitudes and Q^2 dependence of the resonant multipoles for the electroproduction of the Δ.

* By experimental we mean that the expression follows the convention of Hand[11] for inclusive electroproduction cross sections. For details, see Dombey.[12]

While it may be that specific features of the model, such as the truncation of the harmonic oscillator basis, are among the sources of the problem, it appears at first sight, that a large contribution to the discrepancy comes from the use of the radiation potential for real photons to describe the interaction with virtual photons. As it is well known, the transformation of this potential, expanded in plane waves, from a four-dimensional to a three-dimensional Fourier integral, is done by the substitution of

$$A_\mu(x) = \frac{1}{(2\pi)^2} \int b_\mu(q) e^{iqx} d^4q \tag{4}$$

in the free-field equation

$$\frac{\partial}{\partial x^\sigma}\frac{\partial}{\partial x_\sigma} A_\mu = \Box^2 A_\mu = 0 \quad . \tag{5}$$

The result is that the Fourier transforms $b_\mu(q)$ have the form $b_\mu(q) = \delta(q^2)c_\mu(\mathbf{q})$, which simplify the integration of the energy part of $A_\mu(x)$, transforming it into a three-dimensional integral with a factor $(1/|\mathbf{q}|)^{1/2}$, because $\delta(q^2)$ is interpreted as $\delta(q_0^2 - |\mathbf{q}|^2)$. It is clear that B–M's replacement of $|\mathbf{q}|$ (or $|\mathbf{q}^*|$ in the c.m.) by K_0 in the factor, is valid for real photons ($Q^2 = 0$,) but may not be so for virtual photons, which obey the condition

$$\Box^2 A_\mu = Q^2 A_\mu \ , \quad Q = \text{imaginary virtual photon mass.} \tag{6}$$

Thus, as originally suggested by Dalitz and Yennie[13] it is the Møller potential that should be used in the treatment of multipole expansions when virtual photons are involved. This potential introduces an extra term for longitudinal (scalar) photons which may lead to improved results.

In addition, it should be kept in mind that as Q^2 increases (and we have followed the model up to $4[\mathrm{GeV/c}]^2$), the validity of a nonrelativistic approach becomes even more questionable than at the photoproduction point.

In fact, the latitude of the approximations involved is such that we may safely say that the real test of the color magnetism model in the context of Δ electroproduction is yet to be carried out, and it will require an improved theoretical treatment as well as more accurate and extensive experimental results, in particular for the scalar and quadrupole moments. In this respect, it should be mentioned in passing , that while exclusive photoproduction and electroproduction experiments will give the final answer, the contribution of new inclusive experiments that could be done in the near future at existing facilities such as the Nuclear Physics program at Stanford Linear Accelerator Center, could resolve some of the more basic outstanding problems for this and other constituent models of the hadrons.

As an illustration of these conclusions, the reader is referred to figs. 5 and 6, which show the results of applying the color magnetism model, with the variation of substituting K_0 *after* the original $(1/|\mathbf{q}^*|)^{1/2}$ has been cancelled with factors of $|\mathbf{q}^*|$ in the matrix elements, to become $\sqrt{|\mathbf{q}^*|}$, in the normalization factor N. The surprising agreement with experiment at low Q^2 was obtained by multiplying the value of $M_{1+}(Q^2)$ times a constant factor to normalize it to the experimental $M_{1+}(0)$.

Figure 7 presents the results for the other multipoles. The substitution used in figs. 5 and 6 was applied once again, to obtain E_{1+} and L_{1+j} which are seen to obey the condition $Lim_{|\mathbf{q}^*|\to 0} E_{1+}/L_{1+} = 1$ very well. On the other hand, in the case of S_{1+} (and $L_{1+\rho}$ as well,) the matrix elements do not introduce any factors of $|\mathbf{q}^*|$, so that the original (B–M's) replacement of $|\mathbf{q}^*|$ with K_0 applies to these multipoles.

In fig. 8 we display the ratio S_{1+}/M_{1+}, with M_{1+} computed following B–M's prescription, and using the same procedure as for fig. 5. The experimental points[14) at low Q^2 seem to agree better with the latter.

In closing, this author would like to thank Prof. Hans Weber and Dr. Kevin Giovanetti for their valuable comments, and my wife, Mirtha, for her patient proofreading. This work was supported by the Department of Energy.

APPENDIX

The notation followed in this paper adheres to the following conventions:

The photon four-vector is represented by q. In the laboratory system, $q = (q_0, \mathbf{q}) = (\nu, \mathbf{q})$. In the γN c.m. system (which is also the πN c.m. system or the Δ rest frame,) $q = (q_0^*, \mathbf{q}^*)$. The invariant quantity $q^2 = -Q^2$ is the photon invariant mass ($\equiv 0$ for real photons).

Gershtein and Dzhikiya obtained the following expressions for the multipoles:

$$M_{1+} = \left(2.024 + 0.062|\mathbf{q}^*|^2/\alpha^2 - 0.0015|\mathbf{q}^*|^4/\alpha^4\right) N \quad , \tag{A1}$$

$$E_{1+} = -\left(6.264 + 0.61|\mathbf{q}^*|^2/\alpha^2 + 0.25|\mathbf{q}^*|^4/\alpha^4\right) \times 10^{-3} N \quad , \tag{A2}$$

with the normalization factor

$$N = \sqrt{\frac{\pi|\mathbf{q}^*|}{6}}(e/m_q)e^{-|\mathbf{q}^*|^2/(6\alpha^2)}a \quad , \tag{A3}$$

where $\mathbf{q}^*$ is the photon momentum in the γN c.m. system, α is a standard "spring" constant in the nonrelativistic quark model, $m_q = M/\mu_p$ is the quark mass, and a is the πN scattering phase factor, which is given in many places, for example in eq. (10) of the notes on $N's$ and $\Delta's$ in the 1974 edition of the Particle Data Tables.[15)]

The symbol α, used as the "spring" constant for the oscillator, serves also as the fine structure constant in eq. (1), where Γ is the width of the Δ.

Gershtein and Dzhikiya use the standard notation[9] for the multipoles E_{1+}, M_{1+}, in terms of the helicity amplitudes A_λ:

$$E_{1+} = \frac{1}{2\sqrt{3}}\left(A_{3/2} - \sqrt{3}A_{1/2}\right); \quad M_{1+} = -\frac{1}{2\sqrt{3}}\left(3A_{3/2} + \sqrt{3}A_{1/2}\right)$$

while IKK use $M = -M_{1+}$ and $E = \sqrt{3}E_{1+}$.

The scalar and longitudinal multipoles used in this paper, resulting from the combination of Bourdeau and Mukhopadhyay's amplitudes with the mixing coefficients of Gershtein and Dzhikiya, are displayed below:

$$S_{1+} = -\sqrt{\frac{2\pi}{|\mathbf{q}^*|}}\left(e/\sqrt{15}\right) e^{-|\mathbf{q}^*|^2/(6\alpha^2)} \left(0.0966\frac{|\mathbf{q}^*|^2}{6\alpha^2} + 0.0082\frac{|\mathbf{q}^*|^4}{36\alpha^4}\right) \quad , \qquad (A4)$$

$$L_{1+j} = \sqrt{\frac{6\pi}{|\mathbf{q}^*|}}\left(|\mathbf{q}^*|e/m_q\right) e^{-|\mathbf{q}^*|^2/(6\alpha^2)} \left(-10.5 + 4\frac{|\mathbf{q}^*|^2}{\alpha^2} + 0.4\frac{|\mathbf{q}^*|^4}{\alpha^4}\right) \times 10^{-4} \quad , \qquad (A5)$$

and

$$L_{1+\rho} = \frac{|\mathbf{q}^*|}{q_o^*} S_{1+} \quad .$$

REFERENCES

1. A. De Rújula, H. Georgi and S. Glashow, Phys. Rev. **D12** (1975) 147; O. W. Greenberg, Phys. Rev. Lett. **13** (1964) 58.

2. N. Isgur and G. Karl, Phys. Lett. **72B** (1977) 109, Phys. Rev. **D18** (1978) 4187, Phys. Rev. **D19** (1979) 1963; N. Isgur, G. Karl and R. Koniuk, Phys. Rev. **D25** (1982) 2394; S. S. Gershtein and G. V. Dzhikiya, Sov. J. Nucl. Phys. **34** (1981) 870; D. Drechsel and M. M. Giannini, Phys. Lett. **143B** (1984) 329.

3. For color magnetism see ref. 2, and in addition: V. Vento, G. Baym and A. D. Jackson, Phys. Lett. **102B** (1981) 97; V. F. Grushin et al., JETP Lett. **39** (1984) 10; for other models: H. Tanabe and K. Ohta, Phys. Rev. **C31** (1985) 5; A. Wirzba and W. Weise, Phys. Lett. **188** (1987) 6; J. Bienkowska, Z. Dziembowski and H. Weber, Phys. Rev. Lett., **59** (1987) 624.

4. G. Cochard and P. Kessler, Nuovo Cimento Lett. **26** (1969) 783; M. Bourdeau and N. Mukhopadhyay, Phys. Rev. Lett. **58** (1987) 976; J. M. Laget, preprint SACLAY–DPh–N–2482, (1987).

5. W. Pfeil and D. Schwela, Nucl. Phys. **B45** (1971) 379; F. A. Berends and A. Donnachie, Nucl. Phys. **B84** (1975) 342; V. A. Get'man, V. M. Sanin, Yu. N. Telegin and S. V. Shalatskii, Sov. J. Nucl. Phys. **38** (1983) 230. The first two preceding references include phase shifts. For the third one, I used phase shifts for the Δ^+ obtained by averaging the parameters for the Δ^{++} and Δ^0 listed in the reference below and following the procedure therein: V. S. Zidell, R. A. Arndt and L. D. Roper, Phys. Rev. D **21** (1980) 1255.

6. R. H. Dalitz and D. G. Sutherland, Phys. Rev. **146** (1966) 1180; W. W. Ash et al., Phys. Lett. **24B** (1967) 165.

7. E. Amaldi, S. Fubini and G. Furlan, *Pion-Electroproduction* (Springer–Verlag, Berlin, 1979), Springer Tracts in Modern Physics **83** 148.

8. J. L. Friar and W. C. Haxton, Phys. Rev. **C31** (1985) 2027.

9. F. Foster and G. Hughes, Rep. Prog. Phys. **46** (1983) 1445.

10. K. Bätzner et al., Phys. Lett. **39B** (1972) 575 (Bonn); S. Stein et al., Phys. Rev. **D12** (1975) 1884 (Photoprod. and SLAC); J. Alder et al., Nucl. Phys. **B46** (1972) 573 (DESY A); W. Bartel et al., Phys. Lett. **28B** (1968) 148 (DESY B).

11. L. N. Hand, Phys. Rev. **129** (1963) 1834.

12. Norman Dombey, Rev. of Mod. Phys. **411** (1969) 236.

13. R. Dalitz and D. Yennie, Phys. Rev. **105** (1957) 1598.

14. K. Bätzner et al., Nucl. Phys. **B76** (1974) 1; R. Siddle et al., Nucl. Phys. **B35** (1971) 93; J. Alder et al., Nucl. Phys. **B46** (1972) 573; R. Haidan, *DESY Report F21-79/03* (1979).

15. Particle Data Group, Phys. Lett. **50B** (1974) 122.

16. Particle Data Group (PDG), Phys. Lett. **170B** (1986) 259. We quote the value of E2/M1 obtained from individual E_{1+}, M_{1+} entries.

17. H. J. Weber and H. T. Williams, private communication, and preprint to be published in Phys. Lett. B.

18. R. Davidson, N. Mukhopadhyay and R. Wittman, Phys. Rev. Lett. **56** (1986) 804.

19. Richard G. Lipes, Phys. Rev. **D5** (1972) 2849.

20. R. G. Moorehouse, *Electromagnetic Interactions of Hadrons*, ed. A. Donnachie and G. Shaw (Plenum, New York, 1978), pp. 112–125.

21. N. C. Mukhopadhyay and R. Davidson, Report of the 1987 Summer Study Group (RPAC III) (CEBAF, Newport News, 1987), p. 558.

TABLE CAPTIONS

TABLE I. A comparison of values for the E2/M1 ratio obtained by partial wave analyses of experimental data[16] and the color magnetism models. Weber and Williams'[17] value is a recent calculation combining color magnetism and OPEP. The value of Davidson et al.[18] is included as an example of a phenomenological calculation. We note also that Isgur, Karl and Koniuk (IKK)[2] use different definitions for E_{1+}, M_{1+} than the usual ones (refer to the appendix).

TABLE II. Values of Im$E_{1+}^{\pi^0}$, Im$M_{1+}^{\pi^0}$ at the resonant mass $W = 1.232$ GeV (or photon energy $K = 335$ MeV). In the last three columns we show the experimental values, extracted via Watson's theorem from the published results of energy independent multipole analyses, at neighboring photon energies. The values for IKK and those in parentheses for G–D were recalculated by the author using the latest PDG values for the quantities in the pion-nucleon decay factor a. These values are used henceforth.

TABLE III. Experimental results and theoretical predictions for the helicity amplitudes for the $\gamma N \rightarrow \Delta$ transition. The IKK and G–D values were explicitly calculated by the author using as input the matrix elements of ref. 2. The relativistic model is a more complete version by R. Lipes[19] of the Feynman, Kisslinger and Ravndal model. The "no tensor" numbers are from Moorehouse's review of quark models applied to radiative baryon decays.[20] The phenomenological figures are from Mukhopadhyay's recent fit to the world multipole data base.[21]

TABLE I.

Author	Particle Data Group	Isgur–Karl Koniuk	Gershtein Dzhikiya	Bourdeau Mukhopadhyay	Weber Williams	Davic et a
E2/M1	-0.013 ± 0.005	-0.0043	-0.0032	-0.0058	-0.014	-0.015 ±

TABLE II.

Author	Isgur–Karl Koniuk	Gershtein Dzhikiya	Pfeil Schwela	Berends Donnachie	Get'n et a
$M^{\pi^0}_{1+}(10^{-3}\ m^{-1}_{\pi^+})$	16.6	17 (15.6)	25.4 ± 0.2	25.6 ± 0.2	25.4 ±
$E^{\pi^0}_{1+}(10^{-3}\ m^{-1}_{\pi^+})$	-0.07	$-0.055(-0.05)$	$\leq -0.07 \pm 0.07$	-0.15 ± 0.13	≤ -0.16

TABLE III.

Helicity Amplitude	PDG	IKK	Nonrelativistic G–D	No tensor	Relativistic Lipes	Phenomenc Mukhopac
$A_{1/2}$	-141 ± 5	-88	-88	-103	-117	-142 to -
$A_{3/2}$	-258 ± 11	-155	-154	-178	-202	-262 to -

FIGURE CAPTIONS

1. (a) The multipoles S_{1+}, L_{1+} calculated by charge (ρ) and current (j) methods, and E_{1+}, as functions of Q^2. The plot extends to the unphysical value $Q^2 = -0.2[\mathrm{GeV/c}]^2$; (b) same as (a), showing the detail of the negative Q^2 region. The additional scale for the horizontal axis represents the $\mathbf{q}^*$ dependence of the multipoles.

2. The low Q^2 part of the L_{1+} multipoles. The plot for L_{1+} calculated using the current approach is shown as plotted in B–M's original paper (without the exponential factor) and in the correct manner.

3. The Q^2 dependence of the magnetic dipole M_{1+}(solid line), and the calculated (dashed line) experimental values[10] of the corresponding form factor G^*_M. The dipole is scaled up by a factor of 100; while the form factor is plotted normalized to $G_D = 3/(1 + Q^2/0.71)^2$. The sources of the experimental data mentioned in the plot correspond in the same order to those listed in the reference.

4. Resonant part of the inclusive transverse σ_T virtual photon absorption cross section in Δ electroproduction, and the ratio σ_S/σ_T, as functions of Q^2. For the transverse cross section we show (reduced by a factor of 100), the results of the color magnetism calculation and the experimental quantity (inclusive measurements only) at several values of Q^2.[10]

5. Same as fig. 3, but with the factor $\sqrt{K_0}$ instead of $|\mathbf{q}^*|/\sqrt{K_0}$.

6. Same as fig. 4, with the convention of fig. 5.

7. Same as fig. 1(a), with the convention of fig. 5 for E_{1+} and L_{1+j}. Note that S_{1+} and $L_{1+\rho}$ remain unchanged.

8. Ratio S_{1+}/M_{1+} as a function of Q^2, in B–M's approach and with the convention of fig. 5, for M_{1+}. The experimental points are from $\pi^0 p$ electroproduction measurements of $Re(S_{1+}M^*_{1+})/|M_{1+}|^2 \simeq S_{1+}/M_{1+}$ at resonance.[14]

The sources of the experimental points are listed in the figure in the same order as in the reference.

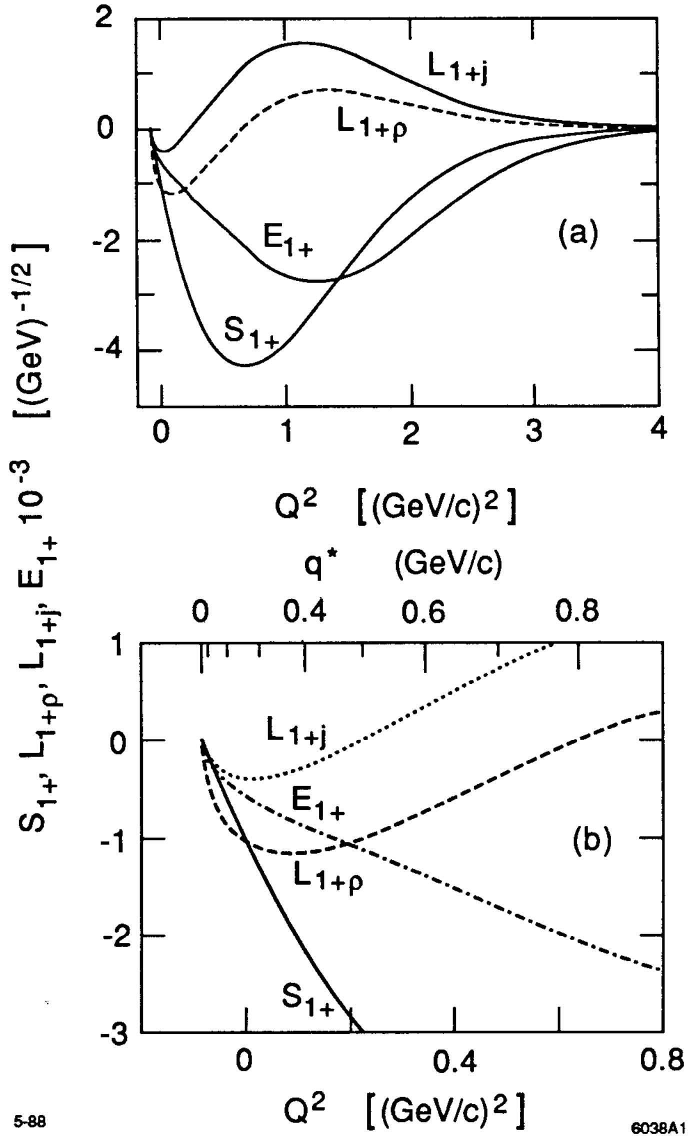
2
0
-2
-4
0
1
2
3
4
L_{1+j}
$L_{1+\rho}$
E_{1+}
S_{1+}
(a)
Q^2 [(GeV/c)^2]
q^* (GeV/c)
0
0.4
0.6
0.8
1
0
-1
-2
-3
L_{1+j}
E_{1+}
$L_{1+\rho}$
S_{1+}
(b)
0
0.4
0.8
Q^2 [(GeV/c)^2]
S_{1+}, $L_{1+\rho}$, L_{1+j}, E_{1+} 10^{-3} [(GeV)$^{-1/2}$]
5-88
6038A1

Fig. 1

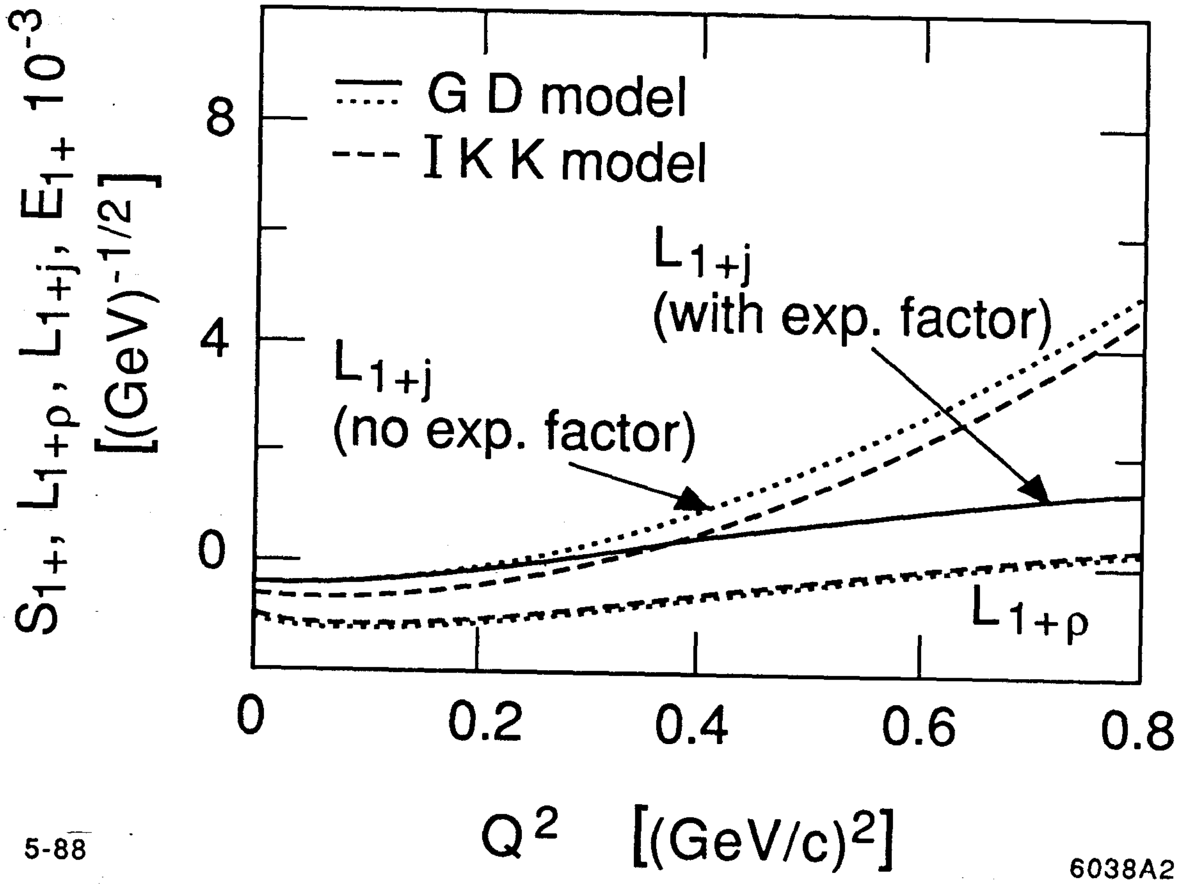

G D model
I K K model
L_{1+j} (with exp. factor)
L_{1+j} (no exp. factor)
$L_{1+\rho}$
8
4
0
0
0.2
0.4
0.6
0.8
$S_{1+}, L_{1+\rho}, L_{1+j}, E_{1+}\ 10^{-3}$ $[(\mathrm{GeV})^{-1/2}]$
Q^2 $[(\mathrm{GeV/c})^2]$
5-88
6038A2

Fig. 2

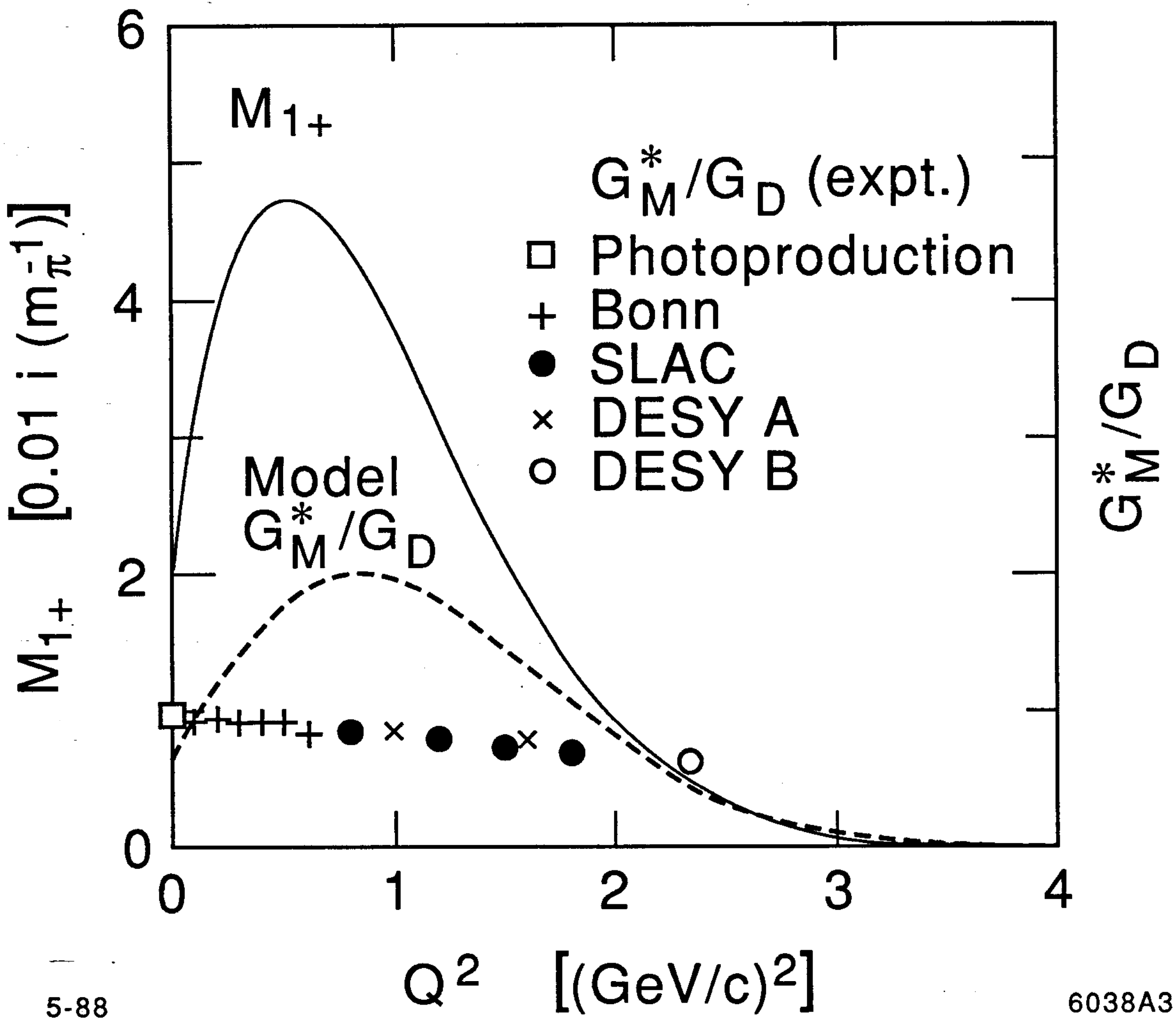

6
4
2
0
0
1
2
3
4
M1+
G*M/GD (expt.)
Photoproduction
Bonn
SLAC
DESY A
DESY B
Model
G*M/GD
M1+ [0.01 i (mπ-1)]
G*M/GD
Q2 [(GeV/c)2]
5-88
6038A3

Fig. 3

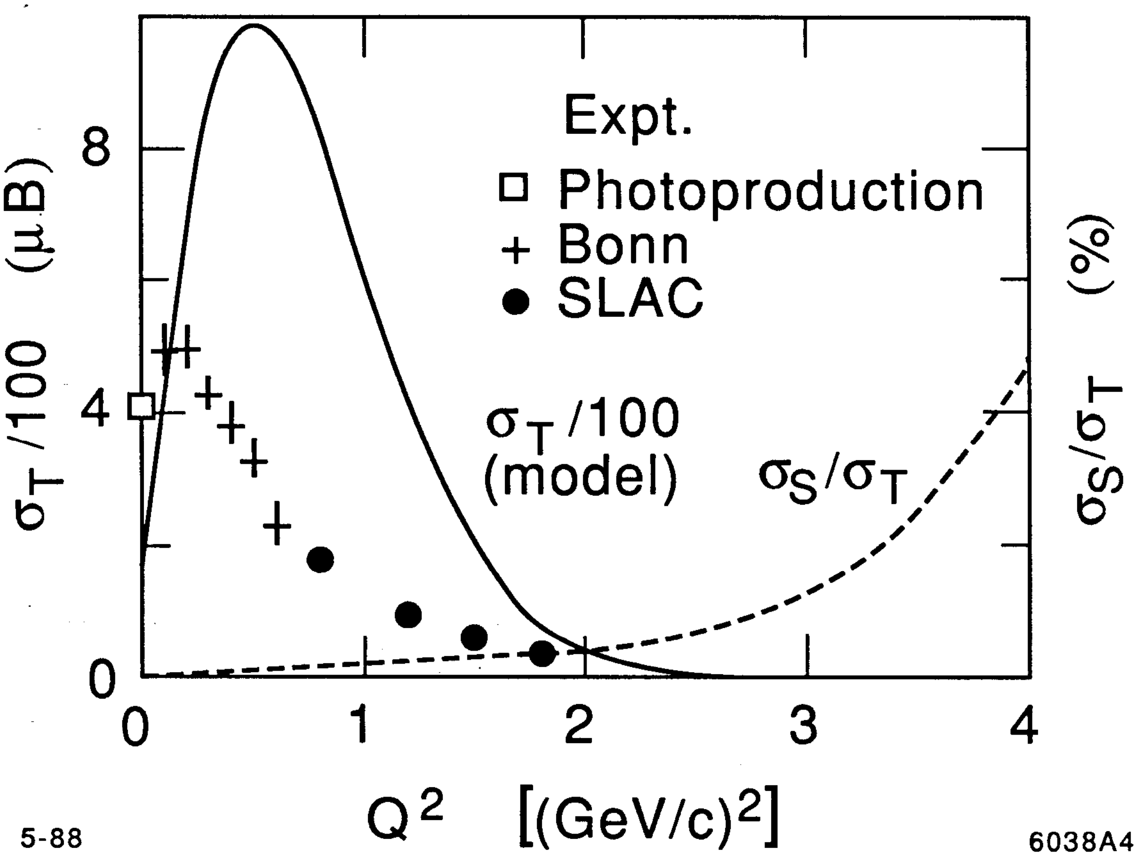
Expt.
Photoproduction
Bonn
SLAC
σ_T/100 (model)
σ_S/σ_T
σ_T/100 (μB)
σ_S/σ_T (%)
Q^2 [(GeV/c)^2]
0
4
8
0
1
2
3
4
5-88
6038A4

Fig. 4

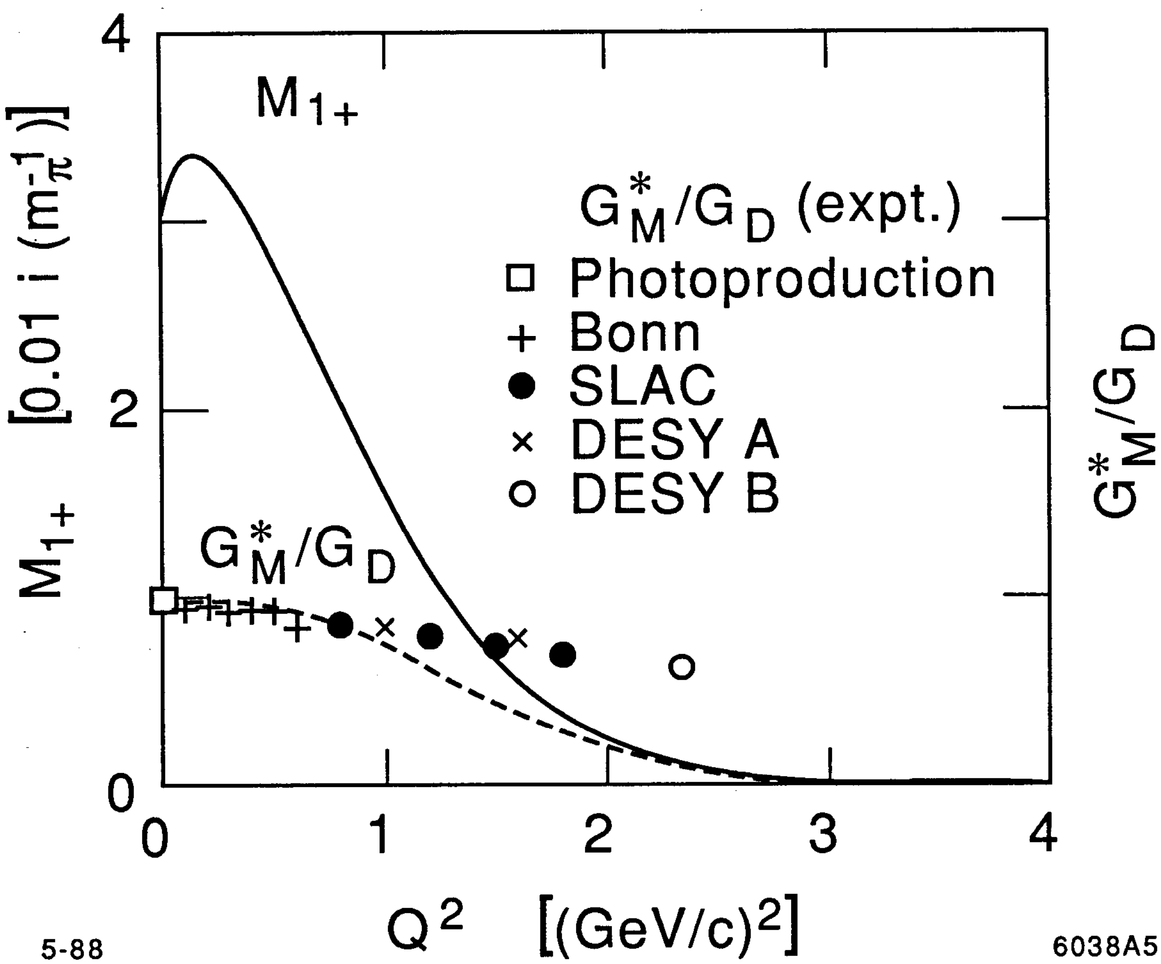

M1+
G*M/GD (expt.)
Photoproduction
Bonn
SLAC
DESY A
DESY B
G*M/GD
M1+ [0.01 i (mπ-1)]
G*M/GD
Q2 [(GeV/c)2]
5-88
6038A5

Fig. 5

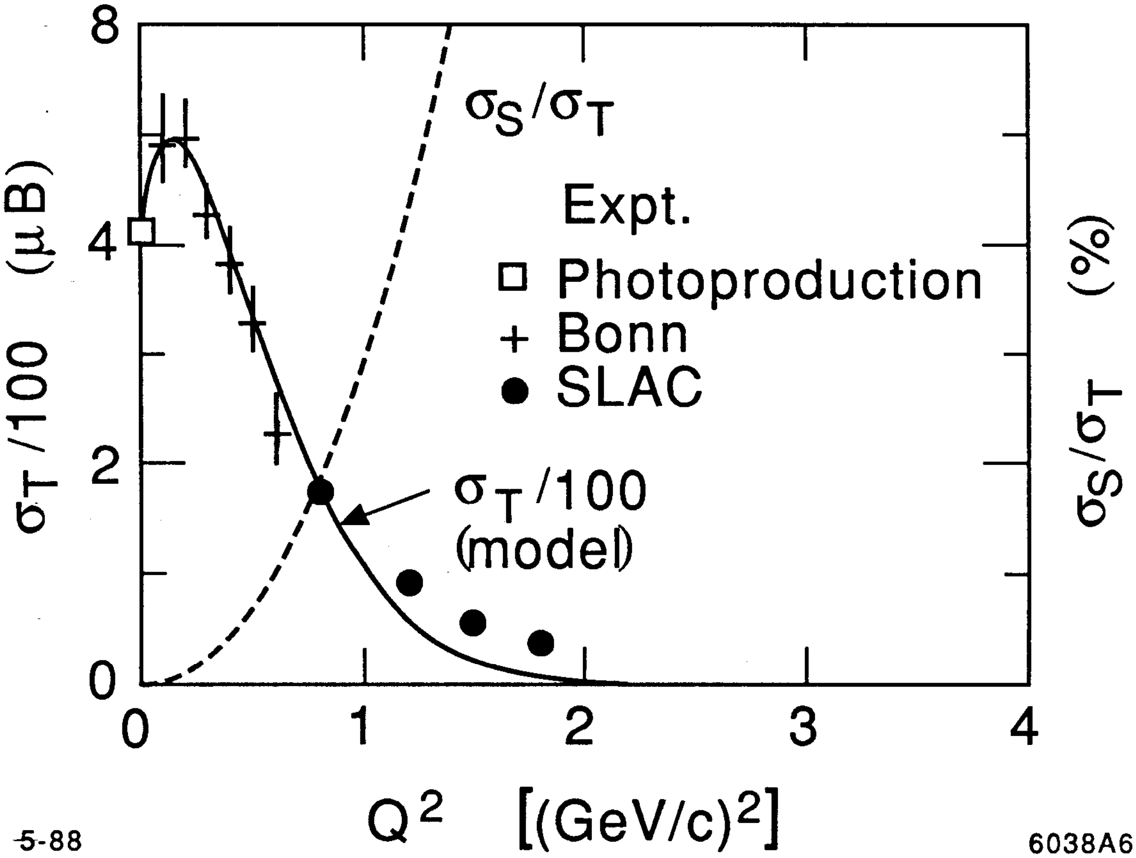
8
4
2
0
0
1
2
3
4
$\sigma_T/100$ (μB)
σ_S/σ_T (%)
σ_S/σ_T
Expt.
Photoproduction
Bonn
SLAC
$\sigma_T/100$
(model)
Q^2 [(GeV/c)^2]
5-88
6038A6

Fig. 6

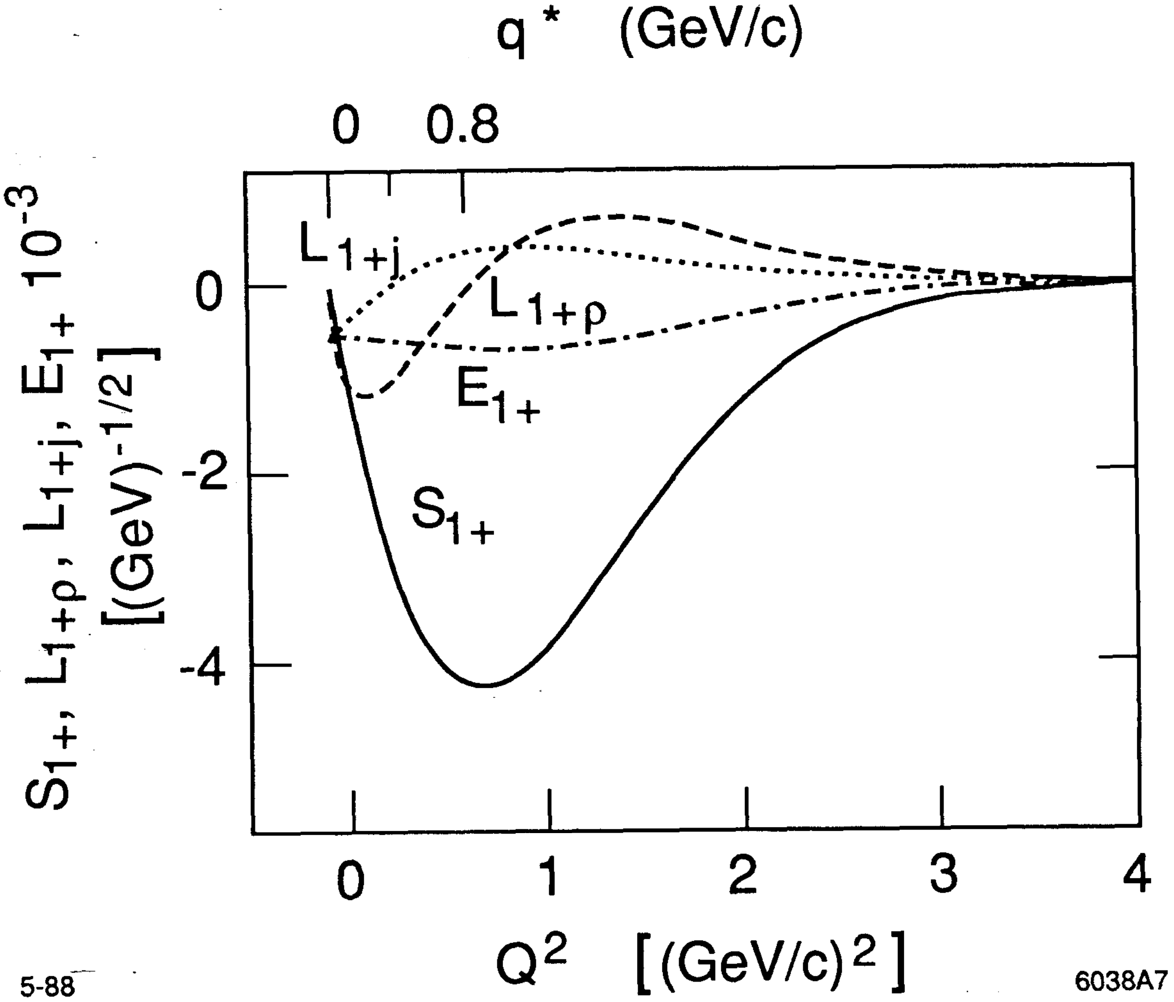
q * (GeV/c)
0
0.8
L 1+j
L 1+ρ
E 1+
S 1+
0
-2
-4
S 1+, L 1+ρ , L 1+j, E 1+ 10-3 [(GeV)-1/2]
0
1
2
3
4
Q2 [(GeV/c)2]
5-88
6038A7

Fig. 7

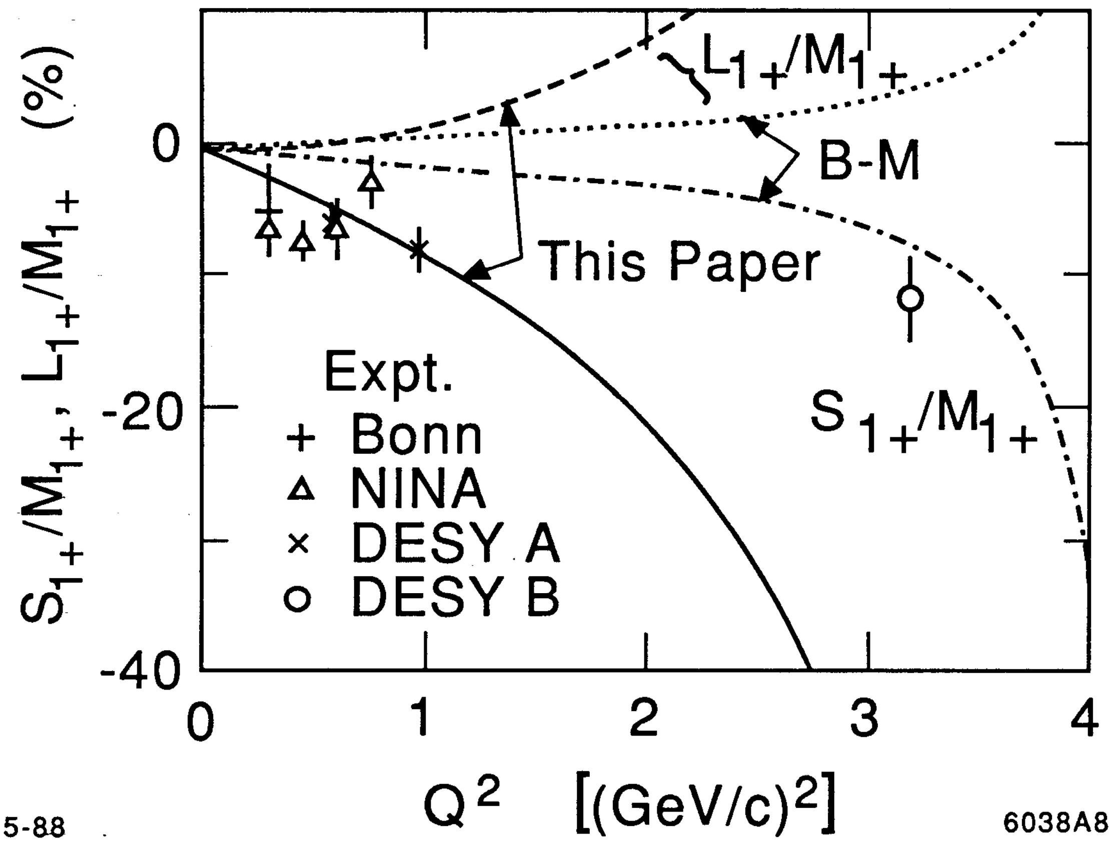

L_{1+}/M_{1+}
B-M
This Paper
S_{1+}/M_{1+}
Expt.
+ Bonn
△ NINA
× DESY A
○ DESY B
S_{1+}/M_{1+}, L_{1+}/M_{1+} (%)
0
-20
-40
0
1
2
3
4
Q^2 $[(GeV/c)^2]$
5-88
6038A8

Fig. 8